ACS OMEGA

Open Access

http://pubs.acs.org/journal/acsodf

Article

Effect of Reaction Conditions on Energy Yield of Pyrolysis Gas from Apple Tree Branches

Haoran Ma, Yanrong Zhang, Ling Qiu, Wulong Li, Renhua Sun, Mingqiang Zhu,* and Xuanmin Yang*

Cite This: *ACS Omega* 2024, 9, 28028−28036

Read Online

ACCESS | Metrics & More | Article Recommendations

ABSTRACT: Although the annual branches of apple trees are substantial, most of them are discarded or incinerated, resulting in a significant waste of resources and environmental pollution concerns. Therefore, it has become necessary and urgent to recycle these branches. Compared with crop straw, apple tree pruning branches exhibit a relatively elevated lignin content, which makes them an optimal feedstock for generating high-quality pyrolysis gases. Energy yield can comprehensively measure the gas production and heat value of the pyrolysis gas. Herein, the effect of reaction conditions on the energy yield of the pyrolysis gas is systematically investigated. The single-factor experimental results show that the optimal conditions are 750 °C reaction temperature, 2 °C/min heating rate, and 120 min holding time. The central composite design test of the response surface establishes that temperature has the most impact, followed by heating rate and holding time. In addition, a regression model is constructed to predict the energy yield of the pyrolysis gas. The analysis of interactions between factors indicates that factors within the lower temperature zones, higher heating rate, and shorter holding time have a more significant influence on the energy yield. These findings provide crucial guidance for the efficient production of pyrolysis gas from apple tree branches.

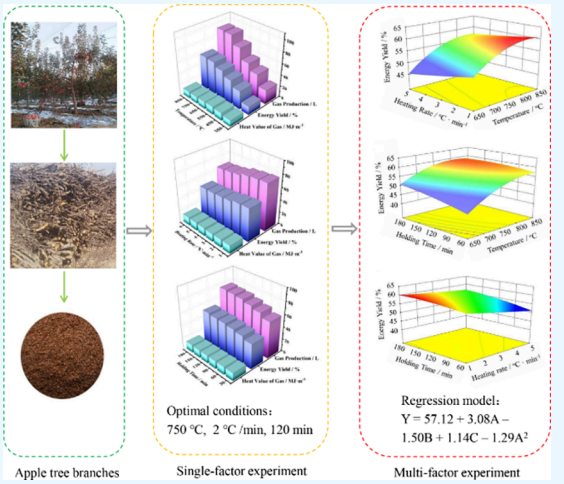

1. INTRODUCTION

Global energy consumption has accelerated rapidly due to the expanding population and economic prosperity.[1,2] The advancement of renewable energy resources (biomass, solar energy, wind energy) has been garnering worldwide attention.[3] Biomass is regarded as a superior renewable resource because of its easy accessibility and zero-carbon emissions. In general, biomass can be converted to high-quality biofuels via various physical, biological, and thermal processes.[4] Among which, pyrolysis emerges as a promising thermal approach owing to its high energy conversion efficiency and economic production.[5] It involves the thermodegradation of biomass into small molecules in an oxygen-deprived environment, engendering the concurrent production of bio-oil, biochar, and pyrolysis gas.[6,7] In particular, bio-oil is a complicated mixture that contains different types of organic compounds.[8] Biochar mainly consists of aromatic hydrocarbons and is composed of about 60% carbon.[9,10] Pyrolysis gas mainly comprises carbon dioxide (CO_2), carbon monoxide (CO), methane (CH_4), and hydrogen (H_2).[11] In general, pyrolysis gas typically accounts for about 30% of biomass pyrolysis products with a high heat value of 8−15 MJ/m^3 and a low tar content of less than 10 mg/m^3,[12] which is an ideal alternative for centralized gas supply, heating, or electric power generation in rural areas.[13] Therefore, the use of biomass pyrolysis technology for the production of clean and renewable gas is of great significance in adjusting rural energy structures and achieving carbon neutrality.[14]

The characteristics of pyrolysis products are influenced by various factors, such as temperature, heating rate, and holding time.[15−17] These factors play a crucial role in determining the composition and properties of the pyrolysis products. Demiral and Şensöz[18] conducted a comprehensive study and reported that an elevated temperature significantly increased the yield of pyrolysis gas when hazelnut and lemongrass were used as feedstocks. Xie et al.[19] observed a substantial rise in the yield of pyrolysis gas during the course of cellulose pyrolysis as the temperature ascended from 500 to 700 °C.[20] Additionally, Tang et al.[21] revealed that temperature significantly influences both the quantity and quality of pyrolysis gas produced from waste biomass and plastics. Researchers have conducted in-depth studies to establish the relationship between heating rate

Received: January 28, 2024
Revised: March 27, 2024
Accepted: June 7, 2024
Published: June 20, 2024

Table 1. Characteristics of Apple Tree Branches[a]

proximate analysis (wt%, ad)				ultimate analysis (wt%, ar)					heating value (MJ/kg)
M	A	V	FC	C	O	H	N	S	HHV
5.94	0.53	79.56	13.97	45.93	43.42	6.16	0.55	0.31	18.94

[a]M: moisture; A: ash; V: volatile matter; FC: fixed carbon; ad: air-dried basis; ar: as-received basis.

and the distribution of biomass primary pyrolysis products.[22−24] Despite the remarkable influence of holding time on pyrolysis, numerous studies have mainly focused on understanding the impact of holding time on the properties of the pyrolysis products.[25,26] The comprehensive evaluation of pyrolysis efficiency relies heavily on the energy yield index, which represents the energy conversion of pyrolysis products in a precise and quantitative manner.[27,28] In order to enhance our understanding of the process, it is vital to probe the complex interplay among the temperature, heating rate, and holding time during pyrolysis. This comprehensive investigation could provide crucial insights into pyrolysis gas's energy yield and aid in the design of effective control strategies for the process.

Apple trees are deciduous plants that are commonly grown in both natural habitats and agricultural practices. Their branches, which constitute a significant source of biomass, are often discarded or incinerated, resulting in significant environmental pollution. Unlike crop straws, apple tree branches contain a higher concentration of lignin and cellulose, making them exceptionally suitable for producing high-quality pyrolysis gas.[29−31] Despite its exceptional potential as a biomass pyrolysis feedstock, there is limited research on this specific application. Therefore, the use of apple tree branches as a raw material for biomass pyrolysis could be a valuable strategy for reducing waste and enhancing ecological sustainability.

In this study, the effects of the temperature, heating rate, and holding time on the energy yield of pyrolysis gas derived from apple tree branches were investigated. The single factor experimental approach was employed to determine suitable pyrolysis conditions, and the response surface methodology was subsequently used to analyze the interactions between paired factors on the pyrolysis gas energy yield. In addition, the relationship between significant factor influence areas and energy yields was also elucidated. The results presented herein provide a theoretical framework and technical supervision for process control and quality administration of apple tree branch pyrolysis. By using such branches as feedstock, the sustainable use of agricultural waste resources can be greatly facilitated.

2. MATERIALS AND METHODS

2.1. Materials. Apple tree branches obtained from the Qianxian farm, Shaanxi Province, China, were processed into 1.43−2.36 mm particles by crushing and screening for further experimentation. The proximate analysis of these materials was conducted following the American Society for Testing Materials, including measurements of fixed carbon, volatile matter, moisture content, and ash. Ultimate analysis was carried out on an elemental analyzer (EA3000, EuroVector, Italy), while the higher heating value was determined on a bomb calorimeter (ZDHW-9000, HebiHongke Coal Evaluation Equipment Factory, China). The full results of these analyses are summarized in Table 1.

2.2. Experimental Equipment. The structure of the equipment is schematically shown in Figure 1. The reaction

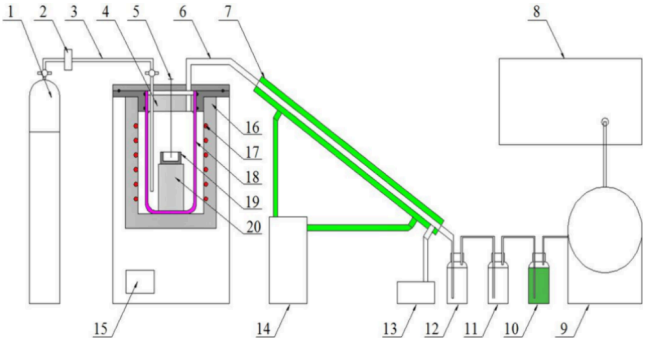

Figure 1. Schematic diagram of biomass pyrolysis equipment: (1) nitrogen cylinder, (2) nitrogen flowmeter, (3) nitrogen pipe, (4) heat insulation plug, (5) thermocouple, (6) outlet pipeline, (7) outer condenser, (8) gas collecting bag, (9) gas flowmeter, (10) gas-washing bottle, (11) refluxing bottle, (12) condensate collecting bottle, (13) vacuum pump, (14) refrigerating machine, (15) controller, (16) ceramic furnace, (17) electric heating device, (18) reaction device, (19) crucible, (20) sample platform.

device (18) employed is a sealed quartz tube having dimensions of 20 cm in diameter and 40 cm in height. Its heating system consists of an electric furnace comprising a ceramic furnace (16) and an electric heating device (17). A sample platform (20) is located at the bottom of the reaction apparatus, where a crucible (19) is placed filled with biomass samples. The biomass sample is fitted with a thermocouple (5) to assess the effective temperature of the pyrolysis reaction. An insulating plug (4) is also placed on the upper part of the reactor. One end of the nitrogen pipe (3) is inserted into the bottom of the reaction apparatus, while the other end is connected to a nitrogen cylinder (1) through a flowmeter (2). The outlet pipe (6) is connected to the upper cover of the reactor, and an outer condenser (7) is welded outside the outlet pipe. The condensed water with a temperature range of 10−15 °C, which is obtained by refrigerating machine (14), circulates in the interlayer between the outlet pipe and the condensation sleeve. The outlet pipe is then connected to a vacuum pump (13). The end of the outlet pipe enters the condensate collection bottle (12), followed by a reflux bottle (11), a gas washing bottle (10), a gas flowmeter (9), and finally a gas collection bag (8). A controller (15) is employed to regulate the temperature, holding time, and heating rate of the pyrolysis reaction. The maximum heating temperature and heating rate of the reactor are 1200 and 10 °C/min, respectively. The combination of these features enables precise and efficient pyrolysis experiments, highlighting the suitability of this laboratory-scale equipment for conducting similar studies

2.3. Experimental Method. The raw material, before being tested, underwent a 12-h drying process in a temperature-regulated blast drying oven at 105 °C. For each

https://doi.org/10.1021/acsomega.4c00911
ACS Omega 2024, 9, 28028−28036

experiment, 100 g of the raw material was placed in a crucible on a sample platform. The reactor was vacuumed first, and then nitrogen was injected at a flow rate of 1 L/min for 0.5 h to ensure an oxygen-free environment. The pyrolysis reaction was then carried out as per the predetermined procedure, and as the temperature increased, the volatile substances were released through the outlet pipe. The condensable components were liquefied and collected in the condensate collection bottle, while the noncondensable components were washed in the gas washing bottle. Gas production was measured by using the gas flow meter and stored in the gas collection bag.

For the single-factor experiment of temperature effect, the raw materials were heated in a controlled mode from room temperature to predetermined temperatures of 350, 450, 550, 650, 750, and 850 °C at a rate of 2 °C/min. The reaction mixture was maintained for 120 min at each temperature, and the temperature was then allowed to cool naturally to room temperature. For the single-factor experiment of heating rate effect, the raw materials were uniformly heated at a rate of 1, 2, 3, 4, 5, and 6 °C/min, until a maximum temperature of 650 °C was reached for a total duration of 120 min. After the target temperature was reached, the materials were allowed to cool naturally. For the single-factor experiment of holding time effect, the raw materials were heated at a uniform rate of 3 °C/min from room temperature to 650 °C. The temperature was maintained for a specific holding time of 30, 60, 90, 120, 150, and 180 min before it was naturally cooled to room temperature.

In order to verify the results of the experiment and ensure the reliability of the experimental data, we carried out the experiments three times under the same conditions. In order to analyze the experimental results, we used SPSS 19.0 software to calculate the standard deviation (SD) of each experimental result. We then compared the experimental results under the same conditions using the *t* test for unpaired values. We chose to report data as mean ± SD because it helps illustrate the distribution of data and is a widely used method in the statistical analysis of data.

2.4. Calculation Method of Energy Yield and Gas Heat Value. The energy yield of pyrolysis gas from apple tree branches was calculated according to eq 1:

$$\text{energy yield}(\%) = \frac{\text{heat value of gas} \times \text{gas production}}{\text{raw material heat value} \times \text{raw material weight}} \times 100\% \quad (1)$$

A foil bag was used to collect pyrolysis gas, which was then subjected to a comprehensive analysis using gas chromatography−mass spectrometry (Agilent 7890 A). Key gases such as CH_4, CO, H_2, and CO_2 were analyzed using the Supelco Carboxen 1010 PLOT column. The heating value of the pyrolysis gas was determined using the average dry gas composition, and the following is shown in eq 2:

$$\text{HV} = (126.36\text{YCO} + 107.98\text{YH}_2 + 358.18\text{YCH}_4 + 629.09\text{YC}_n\text{H}_m) \times 10^{-3} \quad (2)$$

where the *yi* values represent the volumetric proportions of the primary combustible constituents within the dry gases.

3. RESULTS AND DISCUSSION

3.1. Single-Factor Experiment. *3.1.1. Effect of Temperature.* The influence of the temperature on the energy yield, gas production, and gas heat value is shown in Figure 2. The energy yield was calculated based on the combined effects of

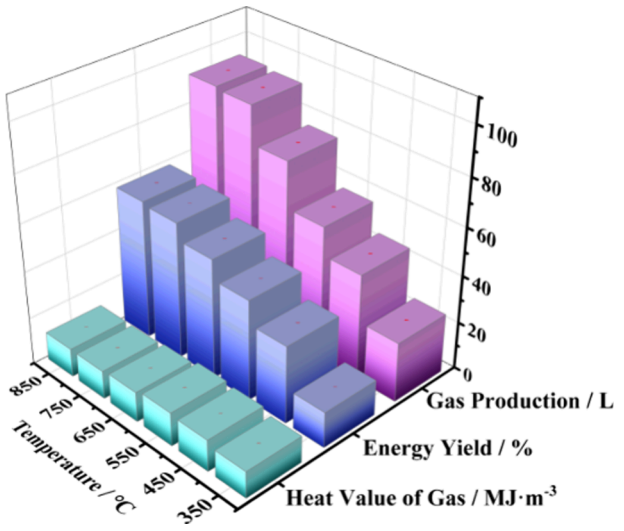

Figure 2. Effect of temperature on heat value of gas, energy yield, and gas production.

gas production and gas heat value. It can be seen that the energy yield increased from 15.06% to 57.84% as the temperature ascended from 350 to 750 °C. However, a further increase in temperature to 850 °C (58.96%) resulted in a marginal increase in energy yield by only 1.12%. A thorough analysis was carried out to investigate the influence of temperature on both gas production and heat value. The pyrolysis gas production increased from 25.24 to 92.67 L as the temperature increased from 350 to 850 °C based on 100 g of apple tree branches, reaching 91.66 L at 750 °C. This phenomenon can be attributed to the decomposition of hemicellulose from 220 to 315 °C, cellulose from 315 to 400 °C, and lignin above 400 °C, leading to the generation of volatile substances during the pyrolysis process.[32] As the temperature continued to rise, the generated volatile substances underwent a secondary reaction, leading to the decomposition of larger molecules into smaller ones.[33] As the temperature continued to rise, the volatile substances produced underwent a secondary reaction, leading to the decomposition of larger molecules into smaller ones. Notably, the magnitude of the secondary reaction increased with the increase in temperature, resulting in a significant increase in gas generation.[34] These findings highlight the critical role of the temperature in the progression of pyrolysis processes, providing valuable insights into the decomposition of plant materials under various temperature conditions.

During the pyrolysis process, the heat value of the resulting gas fluctuates over time as the temperature increases from 350 to 850 °C. Specifically, the heat value of the gas at 350 °C is 11.30 MJ/m^3 and reaches its peak value of 14.23 MJ/m^3 at 550 °C, before plummeting to 12.71 MJ/m^3 at 650 °C. The rate of change in heat value slows down to 12.05 MJ/m^3 at 850 °C. This pattern can be explained by the pyrolysis gas generation process. At approximately 300 °C, depolymerization of holocellulose results in the formation of high oligomers, which are subsequently converted to levoglucosan and light volatiles.[35] At 550 °C, lignin's methyl-containing branched chains pyrolyze, resulting in a significant production of CH_4. Consequently, the methane content reaches its highest point of 19.63% at 550 °C, contributing to the increase in the heat value. On the other hand, as cellulose is decomposed below

https://doi.org/10.1021/acsomega.4c00911
ACS Omega 2024, 9, 28028−28036

350 °C, the cleavage of glycosidic bond produces a substantial amount of CO and CO_2,[36] therefore, the contents of CO_2 (46.48%) and CO (31.76%) reached the maximum value at 350 °C. As the temperature rises above 400 °C, the condensing of aromatic hydrocarbons and the cracking of long-chain hydrocarbons in lignin trigger the production of substantial quantities of H_2. As the temperature increases to 650 °C, a significant number of benzene rings in coke particles undergo dehydrogenation, leading to the formation of polycyclic aromatic hydrocarbons, which in turn contribute to a surge in H_2. In terms of the combined effect of gas production and heat value, the energy yield of pyrolysis gas gradually escalates with an increase in temperature, achieving a peak at 750 °C. Therefore, 750 °C is deemed the optimal temperature for the energy yield of pyrolysis gas from apple tree branches.

3.1.2. Effect of Heating Rate. A systematic study is conducted on the influence of heating rates on the energy yield, gas production, and gas heat value in the pyrolysis of apple tree branches. The results show that the energy yield is negatively affected by an increase in the heating rate (Figure 3). From 1 to 2 °C/min, the energy yield decreased slightly

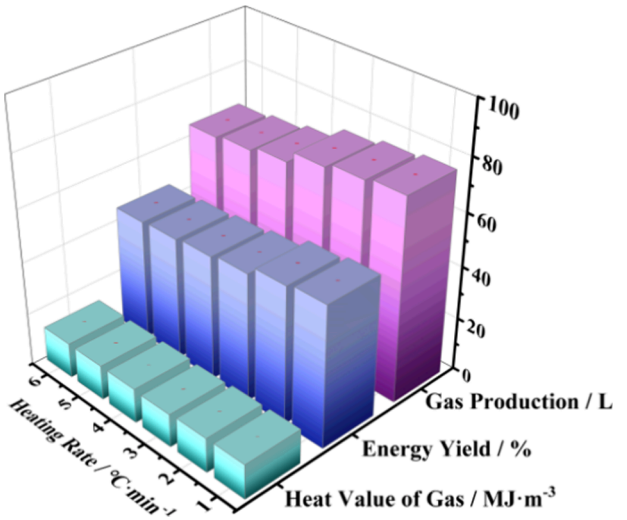

Figure 3. Effect of heating rate on heat value of gas, energy yield, and gas production.

from 53.55% to 52.22%. However, a substantial decline occurred from 3 °C/min to 48.77%. This trend continued from 3 to 6 °C/min, eventually resulting in a total energy yield of 45.83%. At the same time, an increase in the heating rate led to a decrease in gas production. For a sample of 100 g of apple tree branches, the gas production decreased from 76.67 to 65.33 L as the heating rate increased from 1 to 6 °C/min. This phenomenon can be attributed to the rapid heating rate, which impairs the efficient conversion of both internal and external biomass energy,[37] leading to slower volatiles release and thus reduced gas production. Furthermore, a lower heating rate for pyrolysis prolongs the reaction time, allowing organic macromolecules (cellulose, hemicellulose, lignin) to fully decompose.[38,39] On the other hand, an increase in the heating rate from 1 to 6 °C/min slightly elevates the heat value of the gas, from 13.23 to 13.29 MJ/m^3. This shows that the heating rate does not significantly affect the heat value of the gas.

Overall, slower heating rates can increase the energy yield of the pyrolysis gas. However, it is important to note that a lower heating rate also results in a longer reaction time, which, in turn, increases energy consumption throughout the entire process. Furthermore, a change from a heating rate of 2 to 3 °C/min resulted in a significant decrease in energy yield by 3.45%. This indicates that the appropriate heating rate plays a crucial role in promoting efficient pyrolysis. After a comprehensive analysis of the factors mentioned above, a suitable heating rate for obtaining an energy yield of 50% from apple trees' branches is 2 °C/min.

3.1.3. Effect of Holding Time. The graph in Figure 4 shows the influence of the holding time on the energy yield, gas

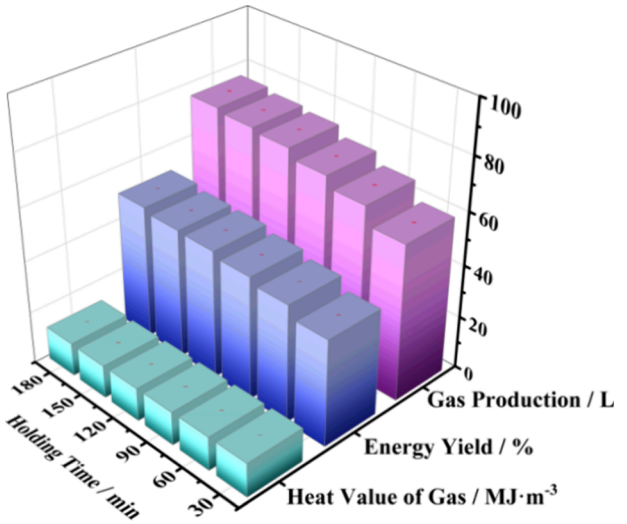

Figure 4. Effect of holding time on the heat value of gas, energy yield, and gas production.

production, and gas heat value. As the holding time extends, the energy yield gradually increases. Specifically, when the holding time is increased from 30 to 120 min, the energy yield increases significantly from 40.54% to 48.99%. Conversely, the increase in holding time from 120 to 150 min resulted in a marginal increase in energy yield, from 48.99% to 49.40%. An increase in holding time to 180 min leads to an energy yield of 51.01%. Consequently, the increase in holding time from 30 to 120 min significantly affects energy yield (by 8.45%), while the increase from 120 to 150 min produces negligible effect (by only 0.41%). Gas production also increases gradually with the extension of holding time. With the holding time extension from 30 to 180 min, the gas production increases from 59.33 to 76.00 L based on 100 g apple tree branches.

As the holding time is prolonged, cellulose undergoes a series of transformations into various dehydrated carbohydrate derivatives, including L-glucose.[40] L-Glucose is one of the most prevalent of these derivatives, with a yield of over 62%.[41] Notably, L-glucose yields carboxylated derivatives throughout the pyrolysis process, which prelude the decarboxylation reaction to generate CO. CO_2 is mainly formed during decarboxylation reactions during pyrolysis of L-glucose. Therefore, a longer holding time facilitates the production of both CO and CO_2. As the holding time increases, the thoroughness of the pyrolysis reaction increases, leading to the production of more noncondensable pyrolysis gases.[42] Despite this, the heat value of the gas remained essentially unchanged regardless of the extension of the holding time, remaining around 12.94 to 12.71 MJ/m^3. A notable feature is that, while a longer holding time does lead to a higher energy yield, it also

https://doi.org/10.1021/acsomega.4c00911
ACS Omega 2024, 9, 28028−28036

requires additional energy input throughout the entire process. Therefore, considering the steady increase in energy yield after 120 min of holding time, it is reasonable to conclude that an optimal holding time for the energy yield of pyrolysis gas from branches would be 120 min.

3.2. Multifactor Experiment. *3.2.1. Model Construction.* In order to thoroughly analyze the energy yield of pyrolysis gas produced from apple tree branches, a robust analytical method called central composite design response surface analysis is used. This is a well-established experimental design methodology that is often used in optimization studies.[43,44] The experimental design includes three independent factors, namely, temperature (A), heating rate (B), and holding time (C), and a single response variable, energy yield (Y). The temperature is chosen to span between 650 and 850 °C, the heating rate varies from 1 to 5 °C/min, and the holding time varies from 60 to 180 min. In addition, the effects of the interactions between these factors on the energy yield are also examined. The experimental factors and codes used are shown in Table 2, while the experimental scheme and the corresponding results of the central composite design are provided in Table 3.

Table 2. Experimental Factors and Codes Used in the Central Composite Design

	factors		
code	A: temp/°C	B: heating rate/°C·min^{-1}	C: holding time/min
1.682	850.00	5.00	180.00
1	809.46	4.19	155.68
0	750.00	3.00	120.00
−1	690.54	1.81	84.32
−1.682	650.00	1.00	60.00

Table 3. Experimental Scheme and Outcomes of the Central Composite Design

entry	A: temp	B: heating rate	C: holding time	Y: energy yield (%)
1	−1	−1	−1	52.55
2	1	−1	−1	58.51
3	−1	1	−1	49.13
4	1	1	−1	57.19
5	−1	−1	1	54.56
6	1	−1	1	59.92
7	−1	1	1	53.48
8	1	1	1	58.46
9	−1.682	0	0	48.39
10	1.682	0	0	58.92
11	0	−1.682	0	61.36
12	0	1.682	0	53.54
13	0	0	−1.682	54.62
14	0	0	1.682	58.47
15	0	0	0	57.55
16	0	0	0	56.15
17	0	0	0	57.59
18	0	0	0	56.45
19	0	0	0	57.53
20	0	0	0	57.36

Based on the test results presented in Table 3, a multiple linear regression analysis is performed using Design Expert software, which yielded a mathematical regression model for the energy yield. The model is expressed by eq 3:

$$Y = 57.12 + 3.08A - 1.50B + 1.14C + 0.22AB - 0.46AC + 0.28BC - 1.29A^2 + 0.051B^2 - 0.27C^2 \quad (3)$$

3.2.2. Model Checking. Design Expert software provides a valuable tool for assessing the significance of the regression coefficient, regression equation, and lack of fit. It is possible to identify the most influential terms and factors contributing to the overall model by assessing their statistical significance. Implementing this approach can lead to a simpler and more efficient model that provides confident predictions of the response variable in the experiment.

Table 4 presents the results of the variance analysis. The single terms A, B, and C and the quadratic term A^2 show exceptional significance ($P < 0.01$). However, interactive items AB, AC, and BC, together with quadratic items B^2 and C^2, show no significant effect ($P > 0.05$). Factors affecting energy yield are analyzed, and their impacts are arranged in descending order: temperature > heating rate > holding time. The regression model has an F value of 23.26 and a P value of <0.001, showing a good fit effect. The F value of the lack of fit is 3.85, and the P value of 0.0825 > 0.05 indicates that the lack of fit is not significant, and the test error is minimal. Therefore, this model could be used as a predictive model for the response value. The minimal test error indicates that the model is reliable for predicting the response value.[45] After discarding the insignificant elements based on the significance test results of the coefficients in Table 4, the simplified model eq 4 is derived.

Table 4. Variance Analysis of the Energy Yield

source	sum of squares	degree of freedom	mean square	F value	P value
A	129.59	1	129.59	132.18	<0.0001
B	30.57	1	30.57	31.18	0.0002
C	17.63	1	17.63	17.98	0.0017
AB	0.37	1	0.37	0.38	0.5528
AC	1.69	1	1.69	1.73	0.2182
BC	0.61	1	0.61	0.62	0.4503
A^2	23.99	1	23.99	24.47	0.0006
B^2	0.038	1	0.038	0.039	0.8476
C^2	1.04	1	1.04	1.06	0.3275
model	205.27	9	22.81	23.26	<0.0001
residual	9.80	10	0.98		
lack of fit	7.78	5	1.56	3.85	0.0825
pure error	2.02	5	0.40		
cor total	215.08	19			

$$Y = 57.12 + 3.08A - 1.50B + 1.14C - 1.29A^2 \quad (4)$$

3.2.3. Effects of Interactions between Factors. 3.2.3.1. Effect of the Interaction between Heating Rate and Temperature on Energy Yield. In Figure 5, a response surface plot and contour map are provided, demonstrating the interaction between the heating rate and temperature on the energy yield. For the factor levels selected in this experiment, the energy yield reaches a minimum when the temperature dips to 650 °C and the heating rate ascends to 5 °C/min. A clear trend emerges as the heating rate escalates from 1 to 5 °C/min; the energy yield diminishes by 6.26%, 5.72%, 5.02%, 4.42%, and 3.81% at temperatures of 650, 700, 750, 800, and 850 °C, respectively. This indicates that the heating rate has a more substantial influence on energy yield in the lower temperature

https://doi.org/10.1021/acsomega.4c00911
ACS Omega 2024, 9, 28028−28036

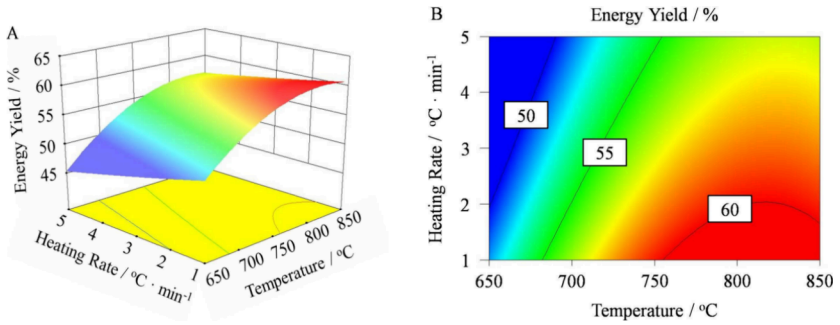

Figure 5. Effect of heating rate and temperature interaction on the energy yield. (A) Response surface plot showing the effect of heating rate and temperature on the energy yield. (B) Contour map showing the effect of heating rate and temperature on the energy yield.

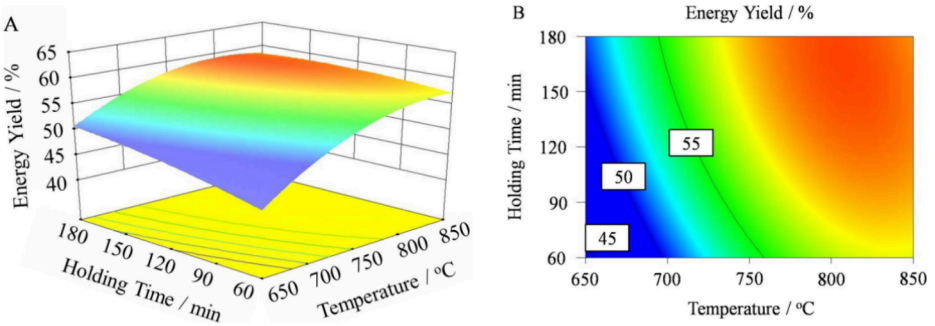

Figure 6. Effect of the holding time and temperature interaction on energy yield. (A) Response surface plot depicting the effect of the holding time and temperature on energy yield. (B) Contour map depicting the effect of the holding time and temperature on energy yield.

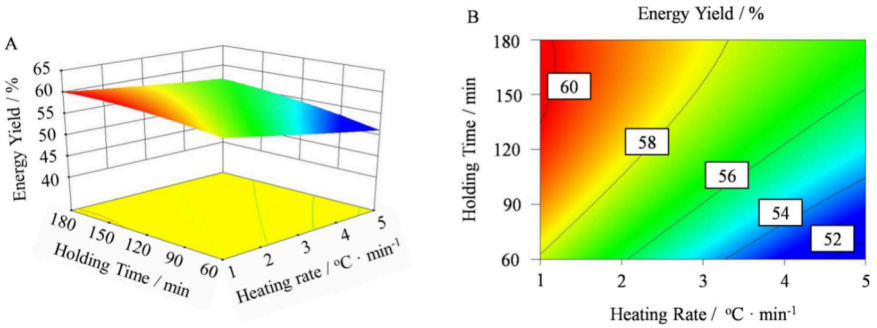

Figure 7. Effect of the holding time and heating rate interaction on energy yield. (A) Response surface plot depicting the effect of the holding time and heating rate on energy yield. (B) Contour map depicting the effect of the holding time and heating rate on energy yield.

range. Conversely, when the temperature ranges from 650 to 850 °C, the energy yield soars by 9.13%, 9.72%, 10.34%, 10.94%, and 11.57% at heating rates of 1, 2, 3, 4, and 5 °C/min, respectively. These findings indicate that temperature plays a significant role in energy yield in the high-heating region. This is likely because rapid heating rates impede volatile diffusion, resulting in nondiffusing substrates participating in deeper pyrolysis reactions, leading to higher energy yield with increasing temperature. In addition, the steepness of the response surface plot and the ellipticity of the contour map are examined to understand the influence of heating rate and temperature on energy yield.[46] The analysis showed that temperature has a greater impact on the energy yield than heating rate. These results contribute to a deeper understanding of the relationship among temperature, heating rate, and energy output in pyrolysis reactions.

3.2.3.2. Effect of the Interaction between Holding Time and Temperature on Energy Yield. As depicted in Figure 6, the response surface plot and contour map vividly illustrate the intricate interplay between holding time and temperature on the energy yield. Within the specified factor level range, a decrease in temperature to 650 °C and a reduction in holding time to 60 min result in a trend toward minimizing energy yield. Conversely, when holding time is extended from 60 to 180 min, there is a gradual and consistent increase in energy yield. Interestingly, the increase in energy yield is noticeably higher in the low-temperature range compared to the high-temperature range, with an increase rate of 6.38% (650 °C) and 1.21% (850 °C), respectively. A similar trend can be observed when the temperature is increased from 650 to 850 °C, with a greater increase rate observed in the lower holding time range. Notably, at 60 min of holding time, the energy yield increases by 12.93%, and at 180 min of holding time, it increases by 7.76%. It is worth noting that extended holding time and elevated temperature are beneficial for both primary and secondary decomposition of biochar residues, leading to a higher degree of pyrolysis and an enhanced energy yield.

https://doi.org/10.1021/acsomega.4c00911
ACS Omega 2024, 9, 28028−28036

3.2.3.3. Effect of the Interaction between Holding Time and Heating Rate on Energy Yield. In Figure 7, we observe the response surface plot and contour map of the effects of the holding time and heating rate on the energy yield. We discover that energy yield tends to be maximized at 60.15% when the heating rate slows down to 1 °C/min and the holding time is extended to 180 min. In contrast, it tends to be minimized at 51.31% when the heating rate increases to 5 °C/min, and the holding time is shortened to 60 min. Moreover, by extending the holding time from 60 to 180 min, the energy yield increases significantly in the higher heating rate range. However, when increasing the heating rate from 1 to 5 °C/min, a significant decrease in energy yield in the lower holding time zone is observed. Specifically, at a holding time of 60 min, the energy yield decreases by 6.57%, while at a holding time of 180 min, the energy yield reduction is only 3.47%. Moreover, the interaction between holding time and heating rate did not have a significant impact on energy yield, which is consistent with variance analysis. These findings provide crucial insights for optimizing the pyrolysis process and enhancing energy yield.

4. CONCLUSIONS

In this study, the influence of the temperature, heating rate, and holding time on the energy yield of pyrolysis gas derived from apple tree pruning branches is studied. It is discovered that the optimal reaction conditions are set at 750 °C, 2 °C/min heating rate, and 120 min holding time. In addition, a regression model is developed to predict the energy yield of pyrolysis gas from apple tree branches. The model is illustrated as $Y = 57.12 + 3.08A - 1.50B + 1.14C - 1.29A^2$. It is revealed that the temperature, heating rate, and holding time all significantly affect the energy yield of pyrolysis gas. The hierarchical order of influence is temperature > heating rate > holding time. This study provides a theoretical basis for the production of highly energetic pyrolysis gas from apple tree pruning branches and provides novel perspectives and references for the energy conversion process of other biomass wastes.

■ ASSOCIATED CONTENT

Data Availability Statement

Data used is available throughout the manuscript text.

■ AUTHOR INFORMATION

Corresponding Authors

Mingqiang Zhu − *College of Mechanical and Electronic Engineering, Northwest A&F University, Yangling, Shaanxi 712100, P. R. China; Western Scientific Observing and Experimental Station for Development and Utilization of Rural Renewable Energy, Ministry of Agriculture and Rural Affairs, Yangling, Shaanxi 712100, P. R. China;* Email: zmqsx@nwsuaf.edu.cn

Xuanmin Yang − *College of Mechanical and Electronic Engineering, Northwest A&F University, Yangling, Shaanxi 712100, P. R. China; Western Scientific Observing and Experimental Station for Development and Utilization of Rural Renewable Energy, Ministry of Agriculture and Rural Affairs, Yangling, Shaanxi 712100, P. R. China;* Email: yangxuanmin@nwsuaf.edu.cn

Authors

Haoran Ma − *College of Chemistry & Pharmacy, Northwest A&F University, Yangling, Shaanxi 712100, P. R. China*

Yanrong Zhang − *College of Chemistry & Pharmacy, Northwest A&F University, Yangling, Shaanxi 712100, P. R. China;* orcid.org/0000-0002-5641-3539

Ling Qiu − *College of Mechanical and Electronic Engineering, Northwest A&F University, Yangling, Shaanxi 712100, P. R. China; Western Scientific Observing and Experimental Station for Development and Utilization of Rural Renewable Energy, Ministry of Agriculture and Rural Affairs, Yangling, Shaanxi 712100, P. R. China*

Wulong Li − *Shaanxi Master of Business Admistration Institute, Xi'an, Shaanxi 710005, P. R. China*

Renhua Sun − *Rural Energy and Environment Agency, Ministry of Agriculture and Rural Affairs, Beijing 100125, P. R. China*

Complete contact information is available at: https://pubs.acs.org/10.1021/acsomega.4c00911

Notes

The authors declare no competing financial interest.

■ ACKNOWLEDGMENTS

This work is supported by Shaanxi Key R&D Program (2022NY-086), Xianyang Key R&D Program (L2023-ZDYF-XCZX-003), Xian yang Qin chuang yuan Science and Technology Innovation Project (L2022-QCYZX-GY-016), and Agricultural Key-scientific and Core-technological Project of Shaanxi Province (2023NYGG011).

■ REFERENCES

(1) Lee, S.; Jung, S.; Kwon, E. E. Catalytic pyrolysis for upgrading silver grass (Miscanthus sinensis) and carbon dioxide into flammable gases. *Bioresour. Technol.* **2022**, *365*, No. 128153.

(2) Madlener, R.; Sunak, Y. Impacts of urbanization on urban structures and energy demand: What can we learn for urban energy planning and urbanization management? *Sustainable Cities and Society* **2011**, *1* (1), 45−53.

(3) Cho, H. H.; Strezov, V.; Evans, T. J. A review on global warming potential, challenges and opportunities of renewable hydrogen production technologies. *Sustainable Materials and Technologies* **2023**, *35*, e00567.

(4) Saravanakumar, A.; Vijayakumar, P.; Hoang, A. T.; Kwon, E. E.; Chen, W. H. Thermochemical conversion of large-size woody biomass for carbon neutrality: Principles, applications, and issues. *Bioresour. Technol.* **2023**, *370*, No. 128562.

(5) Kaur, R.; Kumar, A.; Biswas, B.; Krishna, B. B.; Bhaskar, T. Investigations into pyrolytic behaviour of spent citronella waste: Slow and flash pyrolysis study. *Bioresour. Technol.* **2022**, *366*, No. 128202.

(6) Aravind, S.; Kumar, P. S.; Kumar, N. S.; Siddarth, N. Conversion of green algal biomass into bioenergy by pyrolysis. A review. *Environmental Chemistry Letters* **2020**, *18* (3), 829−849.

(7) Li, X.; Peng, B.; Liu, Q.; Zhang, H. Microwave pyrolysis coupled with conventional pre-pyrolysis of the stalk for syngas and biochar. *Bioresour. Technol.* **2022**, *348*, No. 126745.

(8) Ravikumar, C.; Senthil Kumar, P.; Subhashni, S. K.; Tejaswini, P. V.; Varshini, V. Microwave assisted fast pyrolysis of corn cob, corn stover, saw dust and rice straw: Experimental investigation on bio-oil yield and high heating values. *Sustainable Materials and Technologies* **2017**, *11*, 19−27.

(9) Thakkar, J.; Kumar, A.; Ghatora, S.; Canter, C. Energy balance and greenhouse gas emissions from the production and sequestration of charcoal from agricultural residues. *Renewable Energy* **2016**, *94*, 558−567.

(10) Zhang, C.; Ji, Y.; Li, C.; Zhang, Y.; Sun, S.; Xu, Y.; Jiang, L.; Wu, C. The Application of Biochar for CO2 Capture: Influence of Biochar Preparation and CO2 Capture Reactors. *Ind. Eng. Chem. Res.* **2023**, *62* (42), 17168−17181.
(11) Chen, D.; Li, Y.; Cen, K.; Luo, M.; Li, H.; Lu, B. Pyrolysis polygeneration of poplar wood: Effect of heating rate and pyrolysis temperature. *Bioresour. Technol.* **2016**, *218*, 780−788.
(12) Chen, Y.; Yang, H.; Wang, X.; Zhang, S.; Chen, H. Biomass-based pyrolytic polygeneration system on cotton stalk pyrolysis: influence of temperature. *Bioresour. Technol.* **2012**, *107*, 411−418.
(13) Sun, H.; Feng, D.; Sun, S.; Zhao, Y.; Zhang, L.; Chang, G.; Guo, Q.; Wu, J.; Qin, Y. Effect of acid washing and K/Ca loading on corn straw with the characteristics of gas-solid products during its pyrolysis. *Biomass and Bioenergy* **2022**, *165*, 106569.
(14) Jiang, P.; Zhao, G.; Liu, L.; Zhang, H.; Mu, L.; Lu, X.; Zhu, J. A negative-carbon footprint process with mixed biomass feedstock maximizes conversion efficiency, product value and CO(2) mitigation. *Bioresour. Technol.* **2022**, *351*, No. 127004.
(15) Tang, Q.; Chen, Y.; Yang, H.; Liu, M.; Xiao, H.; Wang, S.; Chen, H.; Raza Naqvi, S. Machine learning prediction of pyrolytic gas yield and compositions with feature reduction methods: Effects of pyrolysis conditions and biomass characteristics. *Bioresour. Technol.* **2021**, *339*, No. 125581.
(16) Zhu, X.; Li, Y.; Wang, X. Machine learning prediction of biochar yield and carbon contents in biochar based on biomass characteristics and pyrolysis conditions. *Bioresour. Technol.* **2019**, *288*, No. 121527.
(17) Yao, Y.; Sun, Y.; Feng, Q.; Zhang, X.; Gao, Y.; Ou, Y.; Yang, F.; Xie, W.; Resco de Dios, V.; Ma, J. Acclimation to nitrogen × salt stress in Populus bolleana mediated by potassium/sodium balance. *Industrial Crops and Products* **2021**, *170*, 113789.
(18) Demiral, İ.; Şensöz, S. Fixed-Bed Pyrolysis of Hazelnut (Corylus AvellanaL.) Bagasse: Influence of Pyrolysis Parameters on Product Yields. *Energy Sources, Part A: Recovery, Utilization, and Environmental Effects* **2006**, *28* (12), 1149−1158.
(19) Xie, S.; Kumagai, S.; Kameda, T.; Saito, Y.; Yoshioka, T. Prediction of pyrolyzate yields by response surface methodology: A case study of cellulose and polyethylene co-pyrolysis. *Bioresour. Technol.* **2021**, *337*, No. 125435.
(20) Iurchenkova, A.; Kobets, A.; Ahaliabadeh, Z.; Kosir, J.; Laakso, E.; Virtanen, T.; Siipola, V.; Lahtinen, J.; Kallio, T. The effect of the pyrolysis temperature and biomass type on the biocarbons characteristics. *ChemSusChem* **2024**, DOI: 10.1002/cssc.202301005.
(21) Tang, Y.; Dong, J.; Zhao, Y.; Li, G.; Chi, Y.; Weiss-Hortala, E.; Nzihou, A.; Luo, G.; Ye, C. Hydrogen-Rich and Clean Fuel Gas Production from Co-pyrolysis of Biomass and Plastic Blends with CaO Additive. *ACS Omega* **2022**, *7* (41), 36468−36478.
(22) Amini, E.; Safdari, M.-S.; DeYoung, J. T.; Weise, D. R.; Fletcher, T. H. Characterization of pyrolysis products from slow pyrolysis of live and dead vegetation native to the southern United States. *Fuel* **2019**, *235*, 1475−1491.
(23) Chen, D.; Chen, X.; Sun, J.; Zheng, Z.; Fu, K. Pyrolysis polygeneration of pine nut shell: Quality of pyrolysis products and study on the preparation of activated carbon from biochar. *Bioresour. Technol.* **2016**, *216*, 629−636.
(24) Zhou, S.; Pecha, B.; van Kuppevelt, M.; McDonald, A. G.; Garcia-Perez, M. Slow and fast pyrolysis of Douglas-fir lignin: Importance of liquid-intermediate formation on the distribution of products. *Biomass and Bioenergy* **2014**, *66*, 398−409.
(25) Norinaga, K.; Shoji, T.; Kudo, S.; Hayashi, J.-i. Detailed chemical kinetic modelling of vapour-phase cracking of multi-component molecular mixtures derived from the fast pyrolysis of cellulose. *Fuel* **2013**, *103*, 141−150.
(26) Solar, J.; de Marco, I.; Caballero, B. M.; Lopez-Urionabarrenechea, A.; Rodriguez, N.; Agirre, I.; Adrados, A. Influence of temperature and residence time in the pyrolysis of woody biomass waste in a continuous screw reactor. *Biomass and Bioenergy* **2016**, *95*, 416−423.
(27) Sahoo, D.; Remya, N. Influence of operating parameters on the microwave pyrolysis of rice husk: biochar yield, energy yield, and property of biochar. *Biomass Conversion and Biorefinery* **2022**, *12* (8), 3447−3456.
(28) Xue, R.; Chi, Z.-Z.; Yang, X.-M.; Qiu, L.; Zhu, M.-Q. Study on the biocontrol efficiency and underlying antagonistic mechanism of valsa canker by pyrolysis tar from apple wood. *Industrial Crops and Products* **2023**, *204*, 117362.
(29) Taboada-Ruiz, L.; Pardo, R.; Ruiz, B.; Díaz-Somoano, M.; Calvo, L. F.; Paniagua, S.; Fuente, E. Progress and challenges in valorisation of biomass waste from ornamental trees pruning through pyrolysis processes. Prospects in the bioenergy sector. *Environmental Research* **2024**, *249*, 118388.
(30) Chen, Y.; Liu, B.; Yang, H.; Wang, X.; Zhang, X.; Chen, H. Generalized two-dimensional correlation infrared spectroscopy to reveal the mechanisms of lignocellulosic biomass pyrolysis. *Proceedings of the Combustion Institute* **2019**, *37* (3), 3013−3021.
(31) Wang, H.; Wang, X.; Cui, Y.; Xue, Z.; Ba, Y. Slow pyrolysis polygeneration of bamboo (Phyllostachys pubescens): Product yield prediction and biochar formation mechanism. *Bioresour. Technol.* **2018**, *263*, 444−449.
(32) Chen, H.; Yang, H.; Ju, F.; Wang, J.; Zhang, S. The influence of pressure and temperature on coal pyrolysis/gasification. *Asia-Pacific Journal of Chemical Engineering* **2007**, *2* (3), 203−212.
(33) Mishra, R. K.; Mohanty, K. Pyrolysis of three waste biomass: Effect of biomass bed thickness and distance between successive beds on pyrolytic products yield and properties. *Renewable Energy* **2019**, *141*, 549−558.
(34) Laird, D. A.; Brown, R. C.; Amonette, J. E.; Lehmann, J. Review of the pyrolysis platform for coproducing bio-oil and biochar. *Biofuels, Bioproducts and Biorefining* **2009**, *3* (5), 547−562.
(35) Cheng, S.; Meng, M.; Xing, B.; Shi, C.; Nie, Y.; Xia, D.; Yi, G.; Zhang, C.; Xia, H. Preparation of valuable pyrolysis products from poplar waste under different temperatures by pyrolysis: Evaluation of pyrolysis products. *Bioresour. Technol.* **2022**, *364*, No. 128011.
(36) Nawaz, A.; Kumar, P. Pyrolysis of mustard straw: Evaluation of optimum process parameters, kinetic and thermodynamic study. *Bioresour. Technol.* **2021**, *340*, No. 125722.
(37) Huang, Q. X.; Wang, R. P.; Zhang, L. J.; Chi, Y.; Yan, J. H. Quantitative Model of Interactions in the Thermal Decomposition of Key Refuse-Derived Fuel Components. *Energy Fuels* **2014**, *28* (2), 1213−1219.
(38) Brown, T. R.; Wright, M. M.; Brown, R. C. Estimating profitability of two biochar production scenarios: slow pyrolysis vs fast pyrolysis. *Biofuels, Bioproducts and Biorefining* **2011**, *5* (1), 54−68.
(39) Park, W. C.; Atreya, A.; Baum, H. R. Experimental and theoretical investigation of heat and mass transfer processes during wood pyrolysis. *Combust. Flame* **2010**, *157* (3), 481−494.
(40) Zheng, A.; Xia, S.; Cao, F.; Liu, S.; Yang, X.; Zhao, Z.; Tian, Y.; Li, H. Directional valorization of eucalyptus waste into value-added chemicals by a novel two-staged controllable pyrolysis process. *Chemical Engineering Journal* **2021**, *404*, 127045.
(41) Patwardhan, P. R.; Satrio, J. A.; Brown, R. C.; Shanks, B. H. Product distribution from fast pyrolysis of glucose-based carbohydrates. *Journal of Analytical and Applied Pyrolysis* **2009**, *86* (2), 323−330.
(42) Mundike, J.; Collard, F. X.; Gorgens, J. F. Pyrolysis of Lantana camara and Mimosa pigra: Influences of temperature, other process parameters and incondensable gas evolution on char yield and higher heating value. *Bioresour. Technol.* **2017**, *243*, 284−293.
(43) Esonye, C.; Onukwuli, O. D.; Ofoefule, A. U. Optimization of methyl ester production from Prunus Amygdalus seed oil using response surface methodology and Artificial Neural Networks. *Renewable Energy* **2019**, *130*, 61−72.
(44) Yuan, X.; Liu, J.; Zeng, G.; Shi, J.; Tong, J.; Huang, G. Optimization of conversion of waste rapeseed oil with high FFA to biodiesel using response surface methodology. *Renewable Energy* **2008**, *33* (7), 1678−1684.

(45) Hasan, M. M.; Rasul, M. G.; Jahirul, M. I.; Khan, M. M. K. Fast pyrolysis of macadamia nutshell in an auger reactor: Process optimization using response surface methodology (RSM) and oil characterization. *Fuel* **2023**, *333*, 126490.
(46) Nawaz, A.; Kumar, P. Thermocatalytic pyrolysis of Sesbania bispinosa biomass over Y-zeolite catalyst towards clean fuel and valuable chemicals. *Energy* **2023**, *263*, 125684.

https://doi.org/10.1021/acsomega.4c00911
ACS Omega 2024, 9, 28028−28036